Two-Dimensional Correlation Analysis in Application to a Kinetic Model of Parallel Reactions

THOU-LONG CHIN and KING-CHUEN LIN*

Department of Chemistry, National Taiwan University, and Institute of Atomic and Molecular Sciences, Academia Sinica, Taipei 106, Taiwan, Republic of China

By applying generalized two-dimensional (2D) correlation analysis as reported by Noda, we have systematically studied a kinetic model of parallel reactions. Given the related rate constants and absorption coefficients, the correlation between reactant and products are analyzed. The reactant–reactant, reactant–product, and product–product pairs are found to be synchronously correlated, and their intensities increase with increase of the rate constant and the absorption coefficient. On the other hand, only the reactant–product pairs show in the asynchronous spectra. Their intensities also depend proportionally on the rate constant and the absorption coefficient. The influence of signal-to-noise ratio (S/N) and overlapped spectra are further discussed. The resulting synchronous and asynchronous correlation spectra for the kinetic model appear to be weakly influenced by poor quality of the signal when the reference spectrum is set at zero. The ratio of asynchronous to synchronous correlation intensity yields a coherence spectrum. This spectrum remains a constant intensity for all the correlated peaks, being free from the influence of rate constant and absorption coefficient as well as being weakly disturbed by a small S/N ratio. It also provides a way to evaluate the extent of spectral overlap between two peaks. The coherence spectrum is useful to characterize the type of parallel reactions.

Index Headings: **Two-dimensional correlation spectrum; Coherence spectrum; Kinetic model; Parallel reaction.**

INTRODUCTION

The basic concept of two-dimensional (2D) correlation infrared (IR) spectroscopy was first introduced more than a decade ago.[1] Given a perturbation-induced time-dependent IR signal, a cross-correlation analysis was used to construct a 2D IR spectrum. The extension of a second dimension provides advantages such as simplification of the complicated spectra with overlapped peaks, enhancement of the spectral resolution, and identification of various intra-molecular and intermolecular interactions through selective correlation of the IR peaks.[1–3] Nevertheless, when the 2D correlation analysis of IR spectroscopy was first reported, the time-dependent IR signal was limited to perturbation of a sinusoidal small amplitude. The method was applied mostly to the vibrational spectral analysis of polymers and liquid crystals as perturbed by mechanical or electrical force.[2–7] In 1993, Noda developed a generalized 2D correlation spectroscopy, which can be applied to analysis of any spectral intensity fluctuations of an arbitrary function of time or any other physical variable.[8] It has become a universal spectroscopy applicable to a very wide range of studies.[9–14]

The 2D correlation plot is obtained by the correlation intensity as a function of two independent spectral variables.[8,13,14] The synchronous correlation intensity characterizes the degree of coherence between two signals that are measured simultaneously. It reaches the maximum if the variations of two dynamic spectra are totally in phase with each other and the minimum if they are antiphase with each other. The peaks along the diagonal line are referred to as autopeaks, of which the correlation intensity corresponds to an autocorrelation of a dynamic spectrum at a particular spectral variable. The peaks located at off-diagonal positions are referred to as the crosspeaks of the dynamic spectra. The crosspeaks reveal the information on the inter- or intra-molecular interactions among the functional groups. On the other hand, the asynchronous correlation intensity indicates the independent or mutually decoupled nature of the dynamic spectra under a perturbation. It becomes the maximum if the two dynamic signals are orthogonal to each other and vanishes if they are in phase or antiphase with each other. The asynchronous correlation spectra consist of only the crosspeaks that are antisymmetric with respect to the diagonal line.[13]

The 2D correlation analysis provides advantages such as those mentioned above. Nevertheless, the change of band position and band width, the baseline shift, and the quality of signal/noise ratio may complicate the interpretation of the correlation spectra.[15–20] The influence of these parameter variations on the 2D correlation spectra has been thoroughly investigated to effectively simplify the resultant contour maps, from which more information may be readily extracted.[15–20]

In this work, we attempt to systematically investigate the 2D correlation analysis for a kinetic model of parallel reactions. Most studies on the kinetic system emphasize the decay behavior of the reactants but are less concerned with the ways to generate the products. In the parallel reactions studied, only one reactant is considered, with three absorption bands, while three different products are involved, each with one absorption band. The 2D correlation spectra are analyzed as functions of reaction rate constant and absorption coefficient. The influence of signal-to-noise (S/N) ratio and the overlapped spectral bands are discussed. Furthermore, when a ratio of asynchronous/synchronous correlation intensity is treated, the resultant coherence spectra appear to be independent of the reaction rate constant and the absorption coefficient. The

Received 8 July 2002; accepted 25 September 2002.
* Author to whom correspondence should be sent.

0003-7028/03/5702-0168$2.00/0

pattern recognition for the parallel reactions becomes significant.

CORRELATION ANALYSIS

The generalized 2D correlation analysis may be applied to any signals fluctuating as an arbitrary function of time or any other physical variable.[8,13] In this work, the 2D correlation analysis is applied to the following parallel reactions:

$$\begin{aligned} A_1 &\xrightarrow{k_{12}} A_2 \\ A_1 &\xrightarrow{k_{13}} A_3 \\ &\vdots \\ A_1 &\xrightarrow{k_{1n}} A_n \end{aligned} \tag{1}$$

where k_{ij} indicates the corresponding rate constant for the species A_i to form A_j. The concentration changes can be monitored by molecular absorption spectroscopy at a particular spectral variable, v_i. The integrated form of the concentration of the reactant A_1 and the products A_j (j = 2, 3, . . . n) may be readily obtained. The concentration change of each species is characterized by a form of exponential function. For conversion of 2D correlation, the dynamic spectral intensity $y(v_1, t)$ at the absorption spectral variable v_1 is first Fourier transformed to yield $Y_1(w)$; w is the Fourier frequency. The conjugate of the Fourier transform, $Y_2^*(w)$, of the other dynamic spectral intensity $y(v_2, t)$ observed at the absorption spectral variable v_2 is likewise obtained. Given the Fourier transforms, $Y_1(w)$ and $Y_2^*(w)$, of the dynamic spectral intensities of $y(v_1, t)$ and $y(v_2, t)$, the Fourier frequency-dependent synchronous and asynchronous correlation spectra, so-called cospectrum and quad-spectrum, respectively, may be obtained as:[8,13]

$$\phi_w(v_1, v_2) = \frac{1}{T}[Y_1^{Re}(w)Y_2^{Re}(w) + Y_1^{Im}(w)Y_2^{Im}(w)] \tag{2}$$

$$\psi_w(v_1, v_2) = \frac{1}{T}[Y_1^{Im}(w)Y_2^{Re}(w) - Y_1^{Re}(w)Y_2^{Im}(w)] \tag{3}$$

where Y_i^{Re} *and* Y_i^{Im} indicate the real and imaginary components of the complex variable Y_i; T is the observed period for the dynamic spectral intensities of $y(v_1, t)$ and $y(v_2, t)$. The synchronous and asynchronous correlation spectra, $\Phi(v_1, v_2)$ and $\Psi(v_1, v_2)$, may then be expressed by:

$$\Phi(v_1, v_2) = \frac{1}{\pi}\int_0^\infty \phi_w(v_1, v_2)\, dw \tag{4}$$

$$\Psi(v_1, v_2) = \frac{1}{\pi}\int_0^\infty \psi_w(v_1, v_2)\, dw \tag{5}$$

Note that $\Phi(v_1, v_2)$ and $\Psi(v_1, v_2)$ denote the real and imaginary components, respectively, of the complex 2D correlation intensities of the two dynamic spectral variations.

In this work, a kinetic model of parallel reactions is made up of three elementary steps. The reactant A_1 is assumed to have three absorption bands with absorption coefficients ε_{11}, ε_{12}, and ε_{13} observed at v_{11}, v_{12}, and v_{13}, respectively. For the products A_2, A_3, and A_4, each has one absorption band with a corresponding absorption coefficient of ε_{21}, ε_{31}, and ε_{41} observed at v_{21}, v_{31}, and v_{41}, respectively. The 2D correlation spectra are studied as a result of variation of rate constant, absorption intensity, and the S/N ratio.

For studying the noise effect, a fixed deviation produced by a random number generator was added to each signal point, so that the S/N ratio may be held at different levels. For calculating the S/N ratio, the signal is counted from the averaged baseline to the averaged peak of each spectrum. MATLAB 6.1, implemented on a personal computer, was used to carry out all the correlation analysis. The time evolutions of the reactant and the products were computed numerically by using the Runge–Kutta–Fehlberg method. Then an FFT program was called to Fourier transform these data to the frequency coordinate.

RESULTS AND DISCUSSION

Two-Dimensional Correlation Analysis for a Parallel Reaction System. Given the parallel reactions as in Eq. 1 with three products, the related rate constants k_{12}, k_{13}, and k_{14} are all assumed to be equal to 1 s^{-1}; the absorption spectral variables for the reactant A_1 are at v_{11} = 15, v_{12} = 45, and v_{13} = 55, and those for the products A_2, A_3, and A_4 are at v_{21} = 35, v_{31} = 65, and v_{41} = 85, and the corresponding absorption coefficients are all set at 1. The initial concentration of A_1 is assumed to be 10 000, while the product concentrations are zero. The resulting 2D correlation analysis for synchronous and asynchronous spectra are shown in Fig. 1. In the synchronous correlation contour map, two aspects may be discerned. First, the magnitudes of the synchronous spectra are all positive. Here we consider the reference spectrum to be equal to zero, such that the resulting synchronous peaks become positive. If an arbitrary reference spectrum is taken, then the synchronous peaks may change sign.[15] Second, all the reactant and products exhibit autopeaks in the diagonal line and the reactant–reactant, reactant–product, and product–product pairs show the crosspeaks. When the reactant decreases, the products may increase. The reactant is closely associated with the product. The products are also related to each other. The branching ratio of the product concentrations relies on the ratio of their corresponding rate constants. The intensities of reactant–reactant correlation appear to be stronger than those of reactant–product and product–product correlations.

As shown in Fig. 1, the asynchronous correlation spectrum is composed of reactant–product correlations, which include the 15–35, 15–65, 15–85, 45–35, 45–65, 45–85, 55–35, 55–65, and 55–85 pairs. Their intensities appear to be the same as a result of equal amounts of the related rate constants and absorption coefficients. Since the rising time for all the products are the same, their asynchronous correlations become zero. The absorption spectral variables at 15, 45, and 55 stem from

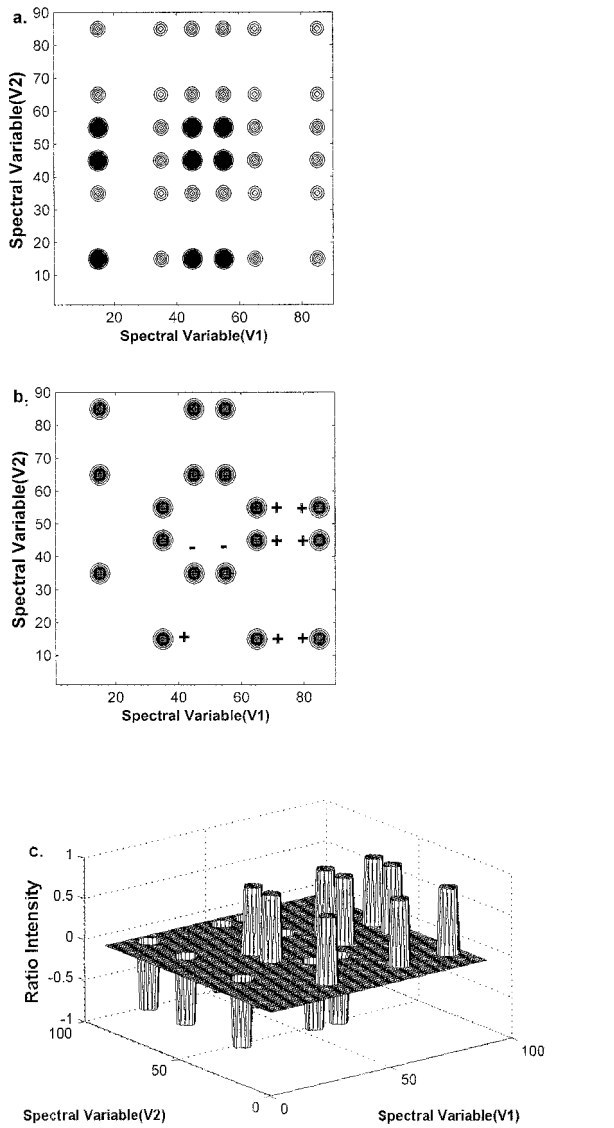

FIG. 1. Contour maps of (**a**) synchronous and (**b**) asynchronous correlation spectra for a kinetic model of parallel reactions. (**c**) Coherence spectra, obtained by the ratio of the asynchronous to synchronous correlation spectra. The absorption spectral variables for the reactant A_1 are at $v_{11} = 15$, $v_{12} = 45$, and $v_{13} = 55$; those for the products A_2, A_3, and A_4 are at $v_{21} = 35$, $v_{31} = 65$, and $v_{41} = 85$. The rate constants $k_{12} = k_{13} = k_{14} = 1$ s^{-1}; the corresponding absorption coefficients are all set at 1.

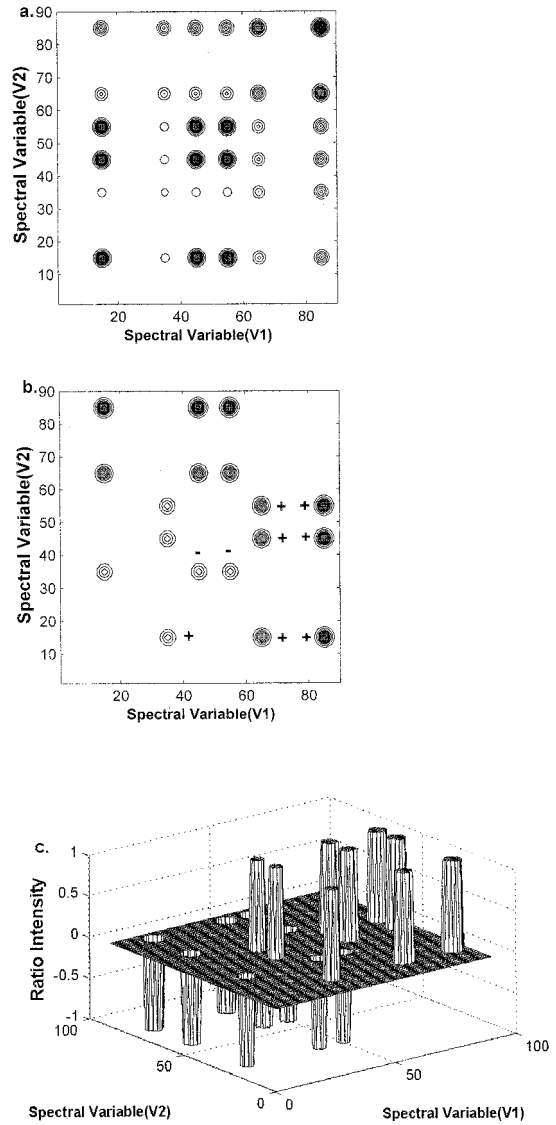

FIG. 2. Contour maps of (**a**) synchronous and (**b**) asynchronous correlation spectra for a kinetic model of parallel reactions. (**c**) Coherence spectra. The conditions are the same as in Fig. 1, except for the rate constants $k_{12} = 1$, $k_{13} = 2$, and $k_{14} = 3$ s^{-1}.

the same reactant A_1, and thus the reactant–reactant asynchronous correlations also disappear. If the ratio of asynchronous to synchronous correlation intensity is treated, the resultant coherence spectrum is made up of cylinder-like peaks with equal intensities for both positive and negative components. The result is also shown in Fig. 1. Note that a blinding filter is used to remove the noise from the asynchronous correlation spectra in the normalization process. The treatment is similar to that used for the global 2D phase map by Ozaki and co-workers.[19] If the asynchronous correlation intensity is smaller than a threshold value, then the weak signal or noise will be ignored. Thus, the 2D pattern of the coherence spectra looks like the asynchronous spectra. The arctangent of the coherence actually corresponds to the global phase angle.[19]

The intensities of synchronous and asynchronous correlations should be subject to the variation of rate constants. We now consider the following case. The rate constants are changed to $k_{12} = 1$, $k_{13} = 2$, and $k_{14} = 3$ s^{-1}, while the absorption coefficients remain the same. As shown in Fig. 2, the product A_4, with a larger rate constant, results in a larger intensity in the synchronous correlation for either autopeaks or crosspeaks, while A_2, with a smaller rate constant, results in a smaller intensity. On the other hand, a larger rate constant such as k_{14} may lead to a larger asynchronous correlation intensity. Therefore, the pairs of 85–15, 85–45, and 85–55 show larger peaks

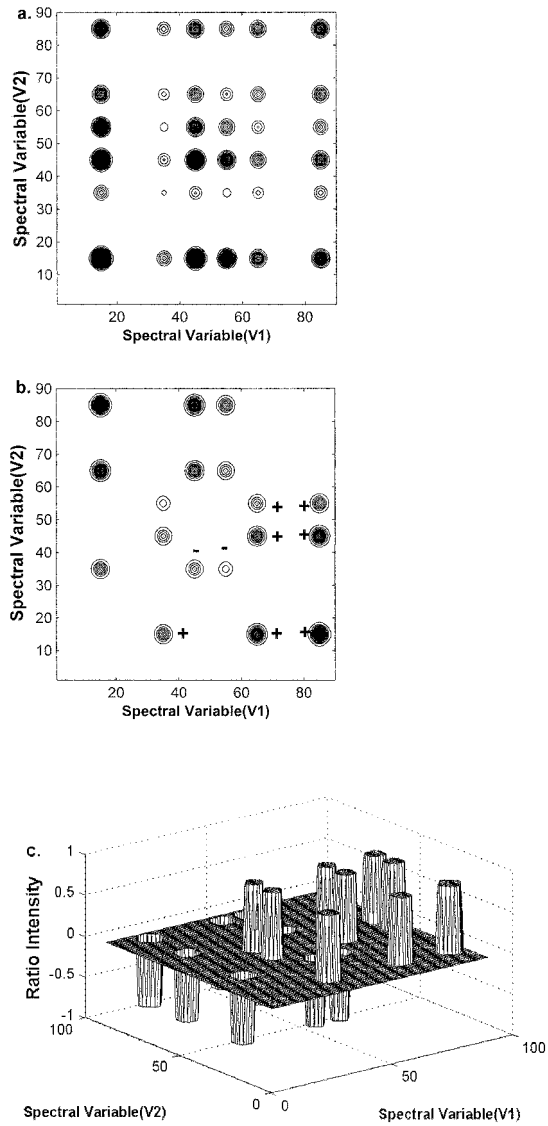

FIG. 3. Contour maps of (**a**) synchronous and (**b**) asynchronous correlation spectra for a kinetic model of parallel reactions. (**c**) Coherence spectra. The rate constants are $k_{12} = 1$, $k_{13} = 2$, and $k_{14} = 3$ s^{-1}. The absorption coefficients for the reactant are changed to $\varepsilon_{12} = 3$ at $v_{12} = 15$, $\varepsilon_{13} = 2$ at $v_{13} = 45$, $\varepsilon_{14} = 1$ at $v_{14} = 55$, and those for the products are changed to $\varepsilon_{21} = 1$ at $v_{21} = 35$, $\varepsilon_{31} = 2$ at $v_{31} = 65$, and $\varepsilon_{41} = 3$ at $v_{41} = 85$.

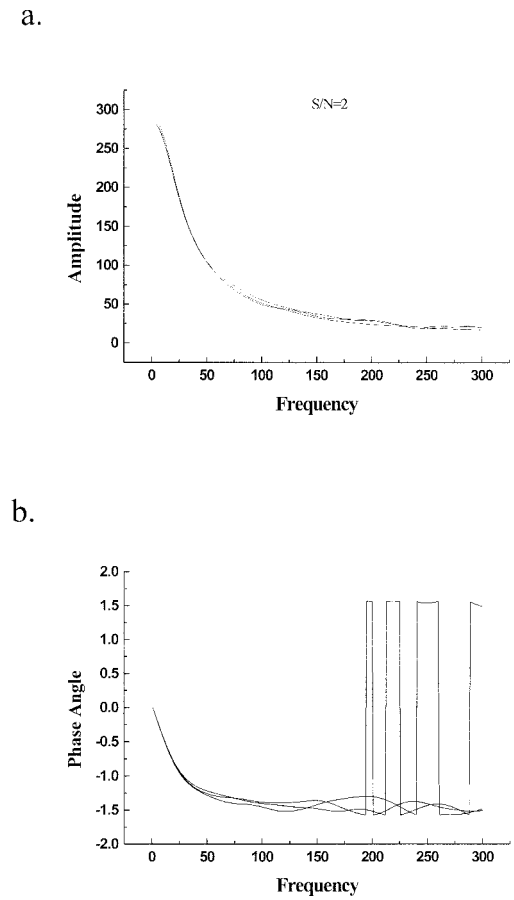

FIG. 4. Noise effect on (**a**) amplitude and (**b**) phase of Fourier transform of $y_1 = \exp(-3t)$ for three replicates under a signal-to-noise (S/N) ratio equal to 2.

than the pairs of 35–15, 35–45, and 35–55. Again, the coherence spectra give rise to cylinder-like peaks with equal intensity, independent of the variation of rate constants.

To understand the influence of the absorption coefficient on the 2D correlation intensities, the rate constants are all fixed at 1 s^{-1}, and then the absorption coefficients for the reactant are changed to $\varepsilon_{12} = 3$ at $v_{12} = 15$, $\varepsilon_{13} = 2$ at $v_{13} = 45$, and $\varepsilon_{14} = 1$ at $v_{14} = 55$, and those for the products are changed to $\varepsilon_{21} = 1$ at $v_{21} = 35$, $\varepsilon_{31} = 2$ at $v_{31} = 65$, and $\varepsilon_{41} = 3$ at $v_{41} = 85$. As shown in Fig. 3, for the synchronous spectrum, the autopeak at 15–15 has the largest intensity. In spite of the same absorption coefficient, the autopeak for the product–product pair at 85–85 (or 65–65 and 35–35) is smaller than that for the reactant–reactant pair at 15–15 (or 45–45 and 55–55). Its interpretation arises from the fact that the depleted amount of reactant is distributed into three channels of products and each channel gains only a fraction. For the crosspeaks, a larger absorption coefficient may lead to stronger correlation intensity. Thus, the reactant–reactant pair at 15–45 yields the strongest intensity, while the reactant–product pair at 55–35 is the weakest. For the asynchronous spectrum, the only existing reactant–product correlation shows that the 15–85 peak is the strongest, while the 35–55 peak is the weakest. Similar to the dependence of the rate constants, the intensities for the 2D correlation spectra are thus subject to the absorption coefficient associated with each correlated pair. The coherence spectrum is also characterized by cylinder-like peaks with equal intensity, which is similar to those in Figs. 1 and 2.

By solving the related equations, we attempt to analyze why the product–product asynchronous spectra disappear and the coherence spectra retain the same peak intensities. For the parallel reactions, the solutions to Eq. 1 give:

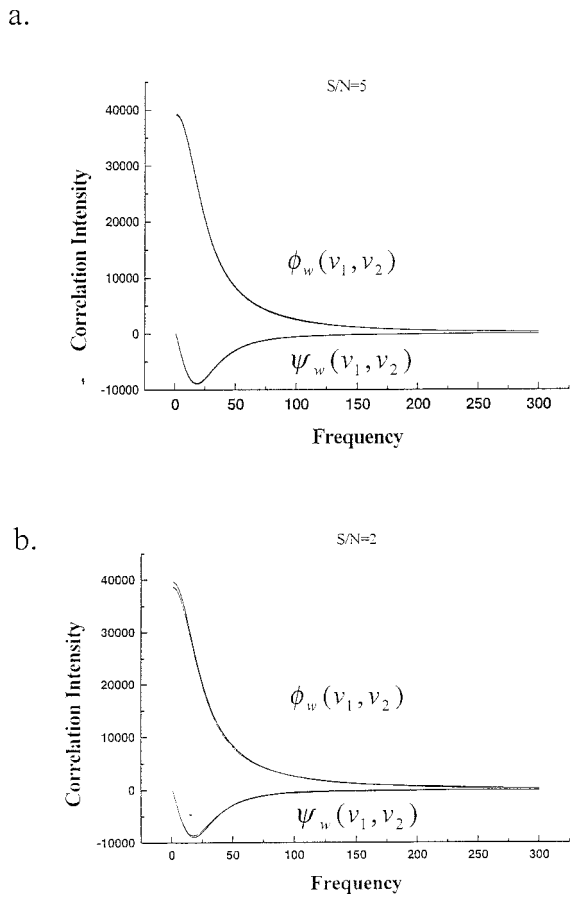

FIG. 5. Comparison of co-spectrum and quad-spectrum correlating the kinetic equations of $y_1 = \exp(-3t)$ and $y_2 = \exp(-7t)$ for three replicates under the conditions of (**a**) S/N = 5 and (**b**) S/N = 2.

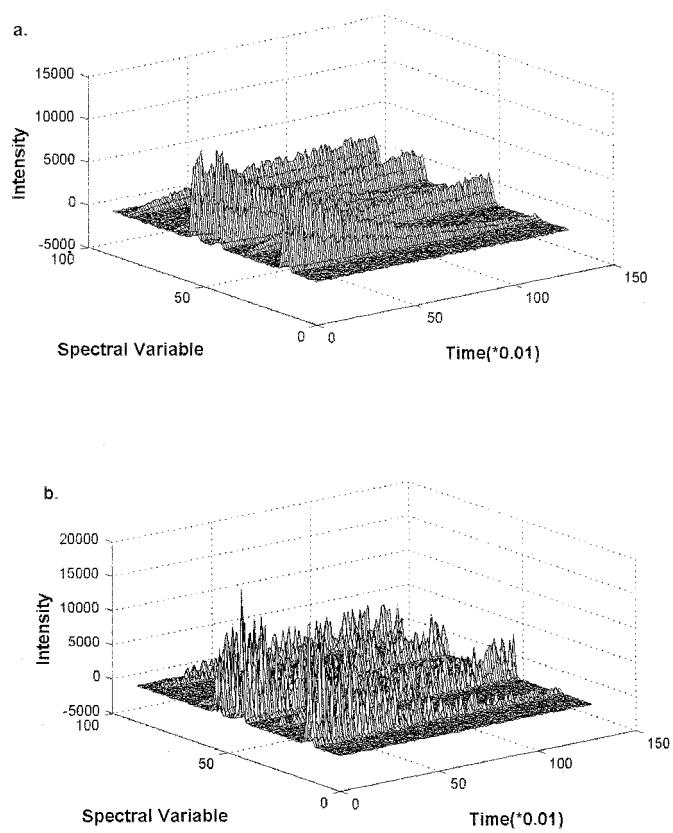

FIG. 6. Time evolution of parallel reactions as described in the text under the conditions of (**a**) S/N = 5 and (**b**) S/N = 1. The related parameters are $k_{12} = 1$, $k_{13} = 1$, $k_{14} = 1$ s^{-1}, $\varepsilon_{12} = 1$ at $v_{12} = 15$, $\varepsilon_{13} = 1$ at $v_{13} = 45$, $\varepsilon_{14} = 1$ at $v_{14} = 55$, $\varepsilon_{21} = 1$ at $v_{21} = 35$, $\varepsilon_{31} = 1$ at $v_{31} = 65$, and $\varepsilon_{41} = 1$ at $v_{41} = 85$.

$$A_1 = A_{10} k_\tau e^{-k_\tau t}$$

$$A_n = \frac{A_{10} k_{1n}}{k_\tau}(1 - e^{-k_\tau t}) \qquad (6)$$

$$k_\tau = \sum_{i=1}^{n} k_{1i} \qquad (7)$$

where A_{10} indicates the initial concentration of the reactant A_1; k_{1i} is the rate constant for $A_1 \rightarrow A_i$ ($i = 2, 3, \ldots n$), and k_τ, a summation of all the individual rate constants of the products, is indicative of the rising rate for the products. Note that all the products have identical k_τ values. It is the same values of k_τ, but not the same values of individual k_{1i} of the products, that lead to the zero intensity of product–product asynchronous peaks. This fact may be realized from Figs. 2 and 3, in which different k_{1i} of products are considered.

Following the Fourier transform of reactant and products, their synchronous and asynchronous correlation may be simplified as:

$$\Phi(v_1, v_n) = k_{1n} A(v_1) A(v_n) B(k_\tau) \qquad (8)$$

$$\Psi(v_1, v_n) = k_{1n} A(v_1) A(v_n) C(k_\tau) \qquad (9)$$

where $A(v_1)$ and $A(v_n)$ are the absorption intensities of the reactant and the product at spectral variable v_1 and v_n, respectively. $B(k_\tau)$ and $C(k_\tau)$ are the k_τ-dependent formulae obtained from the correlation analysis of Fourier transform of A_1 and A_n in Eqs. 6 and 7. The values of k_{1n}, $A(v_1)$, and $A(v_n)$ are obtained by the multiplication of the coefficient terms in Eqs. 6 and 7, remaining the same in the synchronous and asynchronous correlation spectra. Accordingly, the ratio of $\Psi(v_1, v_n)$ to $\Phi(v_1, v_n)$ should give rise to a constant value R, i.e.:

$$R = \frac{C(k_\tau)}{B(k_\tau)} \qquad (10)$$

Noise Effect on Two-Dimensional Correlation Analysis for Parallel Reactions. The poor quality of the obtained spectra may severely affect the reliability of the 2D correlation analysis and complicate the interpretation.[15–19] Before examining the noise effect on the parallel reactions, we demonstrate its influence on the correlation analysis between two kinetic equations, $y(v_1, t) = \exp(-3t)$ and $y(v_2, t) = \exp(-7t)$. When the signal-to-noise ratio (S/N) is assumed to be 2, the amplitude and phase angle of the Fourier transform of $y(v_1, t)$ as a function of the Fourier frequency w for

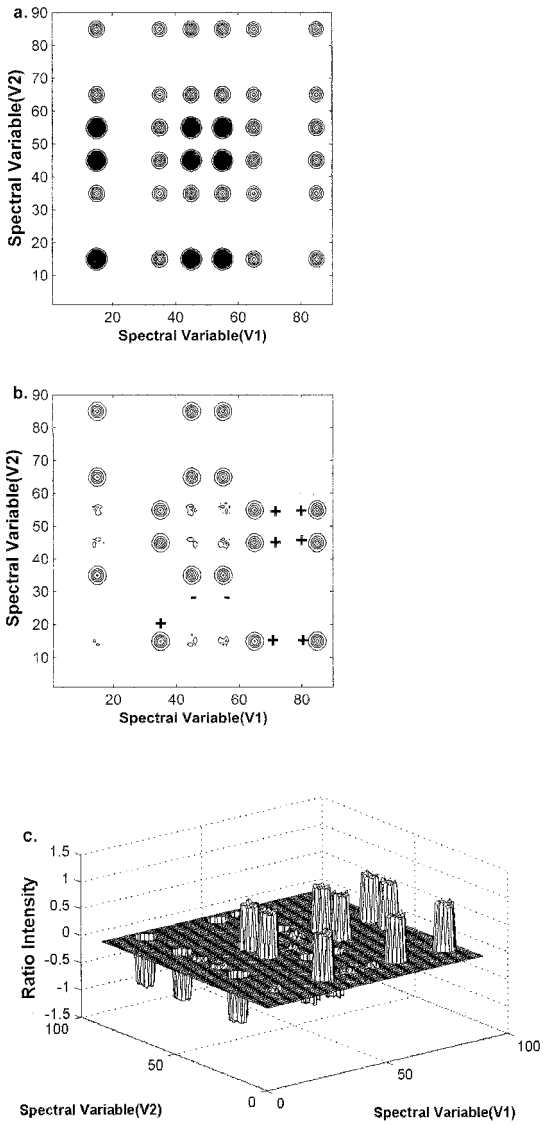

FIG. 7. Contour maps of (**a**) synchronous and (**b**) asynchronous correlation spectra and (**c**) coherence spectra for the parallel reactions given in Fig. 6 under the condition of S/N = 1.

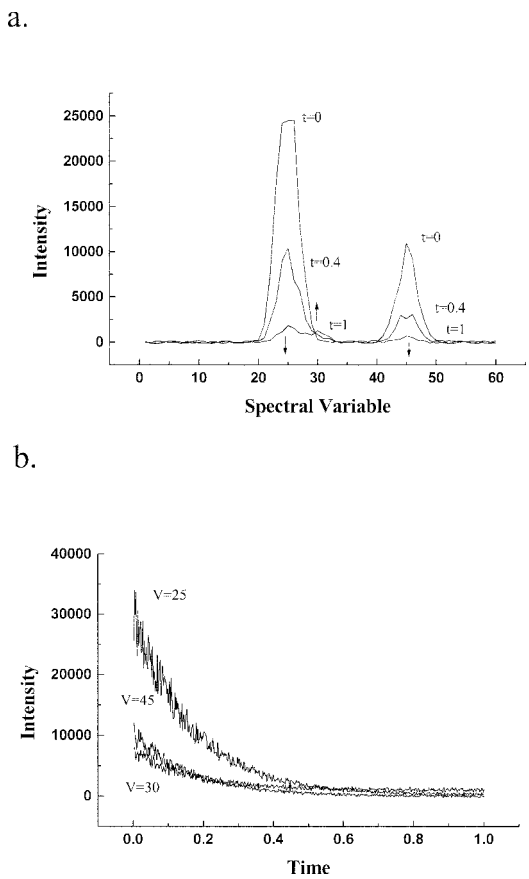

FIG. 8. Time dependence of reactant and product intensity for a kinetic reaction under the condition of S/N = 5 in (**a**) a spectral coordinate and (**b**) a temporal coordinate. The related parameters are $k_{12} = k_{13} = 1\ s^{-1}$, $\varepsilon_{12} = 3$ at $v_{12} = 25$, $\varepsilon_{13} = 1$ at $v_{13} = 45$, and $\varepsilon_{21} = 0.3$ at $v_{21} = 30$.

three replicates are given in Fig. 4. The noise apparently causes severe fluctuation of the phase angle in the region of high-frequency components, at which the amplitudes are very small. Thus, the resulting 2D correlation spectrum becomes slightly affected even with a poor signal quality. Figure 5 shows a comparison for $\phi_w(v_1, v_2)$ and $\psi_w(v_1, v_2)$ between S/N = 2 and 5 for three replicates. They reveal similar qualities for both correlation spectra.

The parallel reactions, made up of the same kinetic equations as in the previous section, are regarded with different S/N ratios for inspection of the noise effect. As the related parameters remain the same as in Fig. 1, the time evolution of reactant and products for S/N = 5 and S/N = 1 are compared in Fig. 6. The decrease of the S/N ratio makes it hard to gain any quantitative information or even discern the type of reaction. However, the corresponding synchronous and asynchronous correlation spectra are surprisingly weakly disturbed by the poor signal quality. Figure 7 shows the case for S/N = 1. The noise-free nature of these correlation spectra has been explained earlier. Furthermore, the coherence spectra (Fig. 7c) give rise to constant intensities for all the correlated peaks, which are also weakly disturbed by the poor S/N ratio. One should note that the reference spectrum is taken as zero in this work. Under this condition, Czarnecki also came to a consistent conclusion that the 2D correlation spectra may be free from heavy distortion of noise and/or baseline fluctuations. While taking an appropriate reference spectrum into account, the number of correlation peaks may be possibly reduced to simply the 2D spectra.[15]

Influence of Overlapped Spectra in Parallel Reactions. The 2D correlation analysis is advantageous to enhance the separation for the overlapped spectral bands. This advantage is also found in the analysis of a kinetic system. Given a simple parallel reaction, the absorption coefficients for the reactant are assumed to be $\varepsilon_{12} = 3$ at $v_{12} = 25$ and $\varepsilon_{13} = 1$ at $v_{13} = 45$, while the absorption coefficient for the product is $\varepsilon_{21} = 0.3$ at $v_{21} = 30$. The rate constants are all assumed to be 1

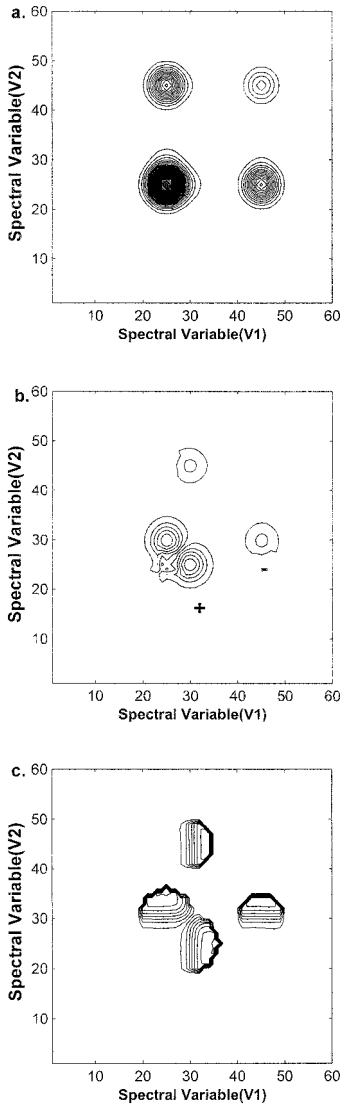

FIG. 9. Contour maps of (**a**) synchronous and (**b**) asynchronous correlation spectra, and (**c**) coherence spectra for the kinetic reaction given in Fig. 8.

s^{-1}. The full width at half-maximum (FWHM) of all the peaks remains 5, with a signal-to-noise ratio at 5. Due to a weak absorption of the product and the severe spectral overlap between $v = 25$ and 30, it is hard to distinguish the product from the reactant, as shown in Fig. 8. After the analysis of 2D correlation, two peaks for the reactant and the product can be clearly recognized at the spectral variable 25 and 30 from the asynchronous correlation spectrum, but not from the synchronous correlation spectrum yielding all the positive peaks (Fig. 9). It may not be easy to evaluate the overlapped region of two peaks from either synchronous or asynchronous correlation spectra. However, when the coherence spectrum is treated, one may easily identify the extent of the spectral overlap from the shaded area of the contour map shown in Fig. 9. The coherence spectrum plays a role of pattern recognition for the type of parallel reactions. The spectrum remains at constant intensity for all the correlated peaks, being free from the influence of the reaction rate constant and absorption coefficient, as well as being weakly disturbed by a poor quality of signal. It also provides a way to evaluate the extent of spectral overlap between two peaks.

CONCLUSION

Two-dimensional correlation analysis has been systematically applied to a kinetic model of parallel reactions. Given the related rate constants and the absorption coefficients, the temporal evolution of reactant and products are determined and their correlations are then analyzed. The reactant–reactant, reactant–product, and product–product pairs are found to be synchronously correlated and their intensities increase with an increase of the rate constant and the absorption coefficient. On the other hand, only the reactant–product pairs show in the asynchronous spectra. The intensities also depend proportionally on the rate constant and the absorption coefficient.

The co-spectra and quad-spectra are analyzed, revealing that the major contribution to the amplitude lies in the low Fourier frequency region. The noise effect results in a marked fluctuation of the phase angle in the high Fourier frequency region. The amplitude contribution in this region is relatively small, such that the resulting 2D synchronous and asynchronous correlation spectra may be weakly influenced by a poor quality of signal. The coherence spectrum retains constant peak intensity, irrespective of a small signal-to-noise ratio and variation of the rate constants and absorption coefficients. This spectrum may well characterize the type of parallel reaction, even when the temporal or spectral-dependent spectra of the species in the reaction are hardly discerned due to serious noise effect or spectral overlap.

ACKNOWLEDGMENT

This work was supported by the National Science Council, Republic of China, under contract no. NSC 90-2113-M-002-036.

1. I. Noda, Bull. Am. Phys. Soc. **31,** 520 (1986).
2. I. Noda, J. Am. Chem. Soc. **111,** 8116 (1989).
3. I. Noda, Appl. Spectrosc. **44,** 550 (1990).
4. I. Noda, A. E. Dowrey, and C. Marcott, Appl. Spectrosc. **42,** 203 (1988).
5. R. A. Palmer, C. J. Manning, J. L. Chao, I. Noda, A. E. Dowrey, and C. Marcott, Appl. Spectrosc. **45,** 12 (1991).
6. C. Marcott, A. E. Dowrey, and I. Noda, Appl. Spectrosc. **47,** 1324 (1993).
7. H. Sasaki, M. Ishibashi, A. Tanaka, N. Shibuya, and R. Hasegawa, Appl. Spectrosc. **47,** 1390 (1993).
8. I. Noda, Appl. Spectrosc. **47,** 1329 (1993).
9. C. Marcott, A. E. Dowrey, and I. Noda, Anal. Chem. **66,** 1065 (1994).
10. M. A. Czarnecki, B. Jordanov, S. Okretic, and H. W. Siesler, Appl. Spectrosc. **51,** 1698 (1997).
11. I. Noda, in *Modern Polymer Spectroscopy,* G. Zerbi, Ed. (Wiley-VCH, Weinheim, 1999), pp. 1–32.
12. N. P. Magtoto, N. L. Sefara, and H. H. Richardson, Appl. Spectrosc. **53,** 178 (1999).

13. I. Noda. A. E. Dowrey, C. Marcott, G. M. Story, and Y. Ozaki, Appl. Spectrosc. **54,** 236A (2000).
14. Y. Ozaki and I. Noda, Eds., *Two-Dimensional Correlation Spectroscopy* (American Institute of Physics, New York, 2000).
15. M. A. Czarnecki, Appl. Spectrosc. **52,** 1583 (1998).
16. P. J. Tandler, P. de B. Harrington, and H. Richardson, Anal. Chim. Acta **368,** 45 (1998).
17. M. A. Czarnecki, Appl. Spectrosc. **53,** 1392 (1999).
18. M. A. Czarnecki, Appl. Spectrosc. **54,** 986 (2000).
19. S. I. Morita, Y. Ozaki, and I. Noda, Appl. Spectrosc. **55,** 1618 (2001).
20. S. I. Morita and Y. Ozaki, Appl. Spectrosc. **56,** 502 (2002).